A TOOL FOR THE AUTOMATED DETECTION OF DAMAGED TRANSPORTATION INFRASTRUCTURE

Sean MacFaden, Research Analyst
Jarlath O'Neil-Dunne, Director
University of Vermont
Spatial Analysis Laboratory
Burlington, VT 05405
smacfade@uvm.edu
joneildu@uvm.edu

ABSTRACT

Remote-sensing imagery has become indispensable to disaster assessment and response, facilitating the analysis of transportation infrastructure damaged by inland flooding, tidal surges, and other natural and anthropogenic events. However, much initial analysis is still performed by manual interpretation of imagery, an effective but laborious process that makes it difficult to assess large areas efficiently and quickly. Object-based image analysis (OBIA) offers a way to automate preliminary assessment of satellite imagery acquired in the immediate aftermath of a disaster, highlighting areas of interest for finer-scale examination and prioritization. To demonstrate the utility of this approach, commercially-available imagery was obtained for two study sites: 1) Longmont, Colorado, which experienced extensive riverine flooding in September 2013; and 2) New York City and adjacent areas, where low-lying coastal areas were flooded by the storm surge associated with Hurricane Sandy in October 2012. For Longmont, an eCognition rule set was developed that identified breaks in the transportation network, including bridge washouts and inundated roads, focusing on the presence of water. For New York City, the rule set focused on transportation disruptions caused by sand and other debris because the storm surge itself had receded by the time the imagery was acquired. To make the rule sets more useful to non-technical end-users, they were adapted for use in eCognition Architect, a software version whose simplified graphic-user interface permits experimentation with classification thresholds using simple slider bars. Identified transportation breaks were exported in multiple formats, including thematic GIS layers and imagery snapshots. To further expedite review of identified breaks, the point location for each break and its accompanying imagery snapshot were displayed in a web-based mapping application. This modeling approach improves transportation disaster response by converting large extent, high-resolution imagery data into information that is easily displayed and interpreted by emergency managers and other practitioners in the field.

KEYWORDS: Disaster, Transportation, OBIA

INTRODUCTION

High-resolution remote-sensing imagery is increasingly important to the evaluation of and response to natural disasters and other catastrophic events, providing an overview of the distribution and severity of damage inflicted on buildings, transportation infrastructure, agriculture, forests, and water resources. For example, recent studies have shown the value of imagery in the aftermath of flooding (Bessis et al. 2004), earthquakes (Bessis et al. 2004, Ehrlich et al. 2009, Voigt et al. 2011), wildfires (Gitas et al. 2008), and volcanic eruptions (Bessis et al. 2004). The timeliness of imagery acquisition is obviously essential to meaningful damage assessment and effective response, as is rapid data distribution to analysts and emergency management officials. Commercial imagery vendors are important sources of timely and comprehensive data, collecting high-resolution imagery at frequent intervals worldwide. Distribution of commercial remote-sensing imagery for use in disaster response analysis and planning is governed by the International Charter for Space and Major Disasters (Bessis et al. 2003, Stryker and Jones 2009), and in the United States it is coordinated by the U.S. Geological Survey through the Hazards Data Distribution System (https://hdds.usgs.gov/hdds2). Implementation of the charter has sometimes proven difficult (Ito 2005), but it nonetheless provides open access to high-quality data that would ordinarily be proprietary.

The techniques used to assess remote-sensing imagery vary widely but often rely on manual interpretation (Ehrlich et al. 2009, Voigt et al. 2011), and indeed crowdsourcing methods dependent on manual review have proven effective following earthquakes in China and Haiti (Barrington et al. 2011). Manual interpretation and crowdsourcing will continue to be important analytical tools in damage assessment, especially with features that are densely

concentrated, such as earthquake-induced damage to buildings in urban neighborhoods. However, manual review of extensive areas remains a difficult task, particularly when damage is broadly distributed and easily overlooked at the moderate scales often used to manually pan over high-resolution imagery. Roads fall into this category; damage to extensive road networks may be widely scattered and highly variable in scope and severity, sometimes including massive road and bridge failures but at other times including less visible impediments such as partial undermining or temporary inundation by water or debris. Disaster-response officials may not have the time or capacity to review massive volumes of data for individual disruptions in road networks, and thus a faster, more efficient method is needed to capitalize on the availability of remote-sensing imagery.

Object-based image analysis (OBIA) offers a method for automating detection of disaster-related road disruptions. An analytical technique that uses expert systems (rule sets) to consider meaningful landscape objects rather than individual pixels (Benz et al. 2004), OBIA is now routinely used with high-resolution imagery for many types of mapping, including feature extraction (O'Neil-Dunne et al. 2014) and comprehensive land cover (MacFaden et al. 2012). Its particular strengths are its ability to incorporate landscape context, or an object's spatial relationships (Benz et al. 2004, O'Neil-Dunne et al. 2011), data fusion (i.e., simultaneous use of multiple raster and thematic vector inputs), and enterprise processing (i.e., simultaneous analysis of multiple tiles). Enterprise processing is especially important for analysis of extensive areas, permitting efficient, fast evaluation of large volumes of data. It can also produce multiple types of GIS-ready output, including raster datasets, vector files, and static snapshots of features of interest. This paper describes an OBIA application for detecting damage to roads inflicted by very different meteorological disasters: 1) inland riverine flooding; and 2) a coastal storm surge. It also demonstrates how high-resolution imagery can be converted into actionable information that is readily usable by disaster-response officials and other end-users who must perform damage-detection analysis with limited time and resources.

METHODS

Data

WorldView-2 imagery was obtained from commercial vendor DigitalGlobe for two study sites affected by major meteorological events: 1) Longmont, Colorado; and 2) New York City. The Longmont area was extensively flooded by rising streams and rivers in September 2013 while the coastal zone in New York City was flooded by a storm surge produced by Hurricane Sandy in October 2012. The floodwaters in both storms significantly disrupted road networks, although the disruptions were different in character. The Longmont floods destroyed roads, wholly or in part, by undermining roadbeds or washing out bridges, or temporarily made them impassable by covering them to a water depth unsafe for automobile traffic. Hurricane Sandy also destroyed transportation infrastructure in some locations, but a more pervasive effect was deposition of sand and other debris by the associated storm surge. The Worldview-2 imagery for both locations was acquired in the immediate aftermath of the storms. Acquired on September 24, 2013, or about 10 days after the worst of the flooding, the WorldView-2 data for Longmont clearly showed breaks in roads and bridges as well as lingering high water covering otherwise intact roads. The data for New York City was acquired on November 4, 2012, about a week after Hurricane Sandy passed through the city, and showed substantial deposits of debris on roads in low-lying coastal zones. The original source imagery provided by DigitalGlobe was available in tiles as 0.5-m panchromatic (450-800nm) and 2-m, 8-band multispectral (Coastal, 400-450nm; Blue, 450-510nm; Green, 510-580nm; Yellow, 585-625nm; Red, 630-690; Red Edge, 705-745; Near Infrared-1, 770-895nm; and Near Infrared-2, 860-1,040nm) imagery that had been geo-referenced but not orthorectified. Using ERDAS Imagine 2011, the panchromatic and multispectral tiles were first mosiacked in the MosaicPro module and then pansharpened using the Hyperspherical Color Space Resolution Merge function. For both study sites, the final pansharpened images had a spatial resolution of 0.5m. Orthorectification was not performed because the study areas had relatively little topographical relief; in addition, orthorectification can be a labor-intensive process that may not be feasible during time-sensitive conditions following a disaster. Statewide road centerline data were obtained from GIS data clearinghouses for both Colorado (http://dtdapps.co.colorado.info/Otis/catalog) and New York (http://gis.ny.gov). Study-area boundaries encompassing pertinent sections of the WorldView-2 imagery datasets were created manually using ArcGIS (ESRI).

Automated Feature Extraction

OBIA processing of post-disaster imagery was performed using eCognition (Trimble); the workflow for automated feature extraction is shown in Figure 1. To accommodate regional differences in the scope and nature of road damage, separate eCognition rule sets were created for the two study areas. For both sites, the first step was to

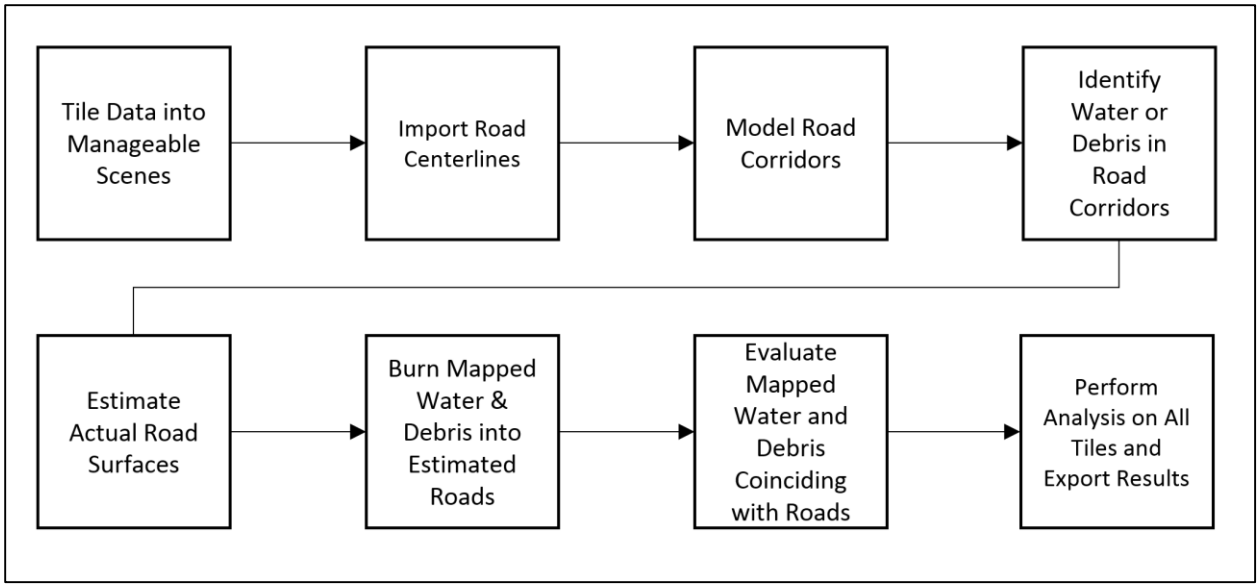

Figure 1. Automated feature extraction steps.

divide the input imagery into reasonably-sized tiles to permit efficient processing. Tiles containing 6,000 x 6,000 pixels with 0.5-meter Worldview-2 imagery worked well, capturing a sufficiently large area to allow for the incorporation of broad-area context-based information without unduly affecting processing speed. The automated process of each tile began by loading the road centerlines and buffering them by a distance of 20m on a side to form a road corridor sufficiently wide to capture roads of most possible widths. The buffer was also used to limit subsequent image segmentation to transportation corridors, expediting processing. For flooding damage in Longmont, Colorado, the next modeling step identified water in the buffered road corridors using a two-step segmentation: 1) Quadtree (Scale, 40; Blue, Green, Red, and Near Infrared-1 bands); and 2) Multiresolution Segmentation Region Grow (Scale, 10; Shape, 0.3; Compactness, 0.8; image layer weights of 1,1,1,2 for Blue, Green, Red, and Near Inrared-1 bands). Objects were then evaluated for the presence of water using the Near Infrared-1 band (<300) and a vegetation index (normalized difference vegetation index, NVDI, <0). Because water may occur adjacent to roads under normal conditions (e.g., bridges, canals, roadside ditches), the classification of water was then refined by estimating actual road surfaces using a pixel-based object resizing process that grew out from the road centerlines. The growing processing halted when road edges reached vegetated objects, water, or other types of impervious surfaces, as evaluated by a combination of NDVI (<0.175) and Visible Brightness (sum of Blue, Green, and Red bands, >1,100). After superimposing previously-mapped water with estimated roads, the identified water features were further evaluated with size and contextual criteria to eliminate small objects that extended beyond the road edge, helping reduce the incidence of false positives. The modeling flow for floodwater-related damage is shown in Figure 2.

For New York City, the overall modeling approach was similar but its rule set evaluated road corridors for the presence of sand and other debris rather than water. Use of simple classification thresholds did not work as well with debris, so a fuzzy classifier incorporating NDVI (distribution, Approximate Gaussian; Min\Max range, 0-0.15); and Visible Brightness (distribution, Approximate Gaussian; Min\Max range, 1,000-2,500) was created instead. This classifier represented a combined probability that objects in roads constituted debris affecting network continuity, and an appropriate cutoff value (0.5) was determined through iterative testing. The modeling flow for debris-related road disruptions is shown in Figure 3.

To facilitate rapid use of this modeling technique by non-technical users, the rule sets for floodwaters and road debris were adapted for use in eCognition Architect, a module that simplifies the rule-based expert system into a graphic-user interface. Architect permits development of slider bars and processing buttons, eliminating direct manipulation of the underlying algorithms. Users thus have the same ability to experiment with modeling criteria but need only focus on the most important variables. For the Longmont, Colorado and New York City rule sets, slider bars were established for the inputs necessary to identify water or debris in road corridors and estimating the actual road surfaces. All other modeling parameters were considered constant. The Architect interface for flood-related damage is shown in Figure 4.

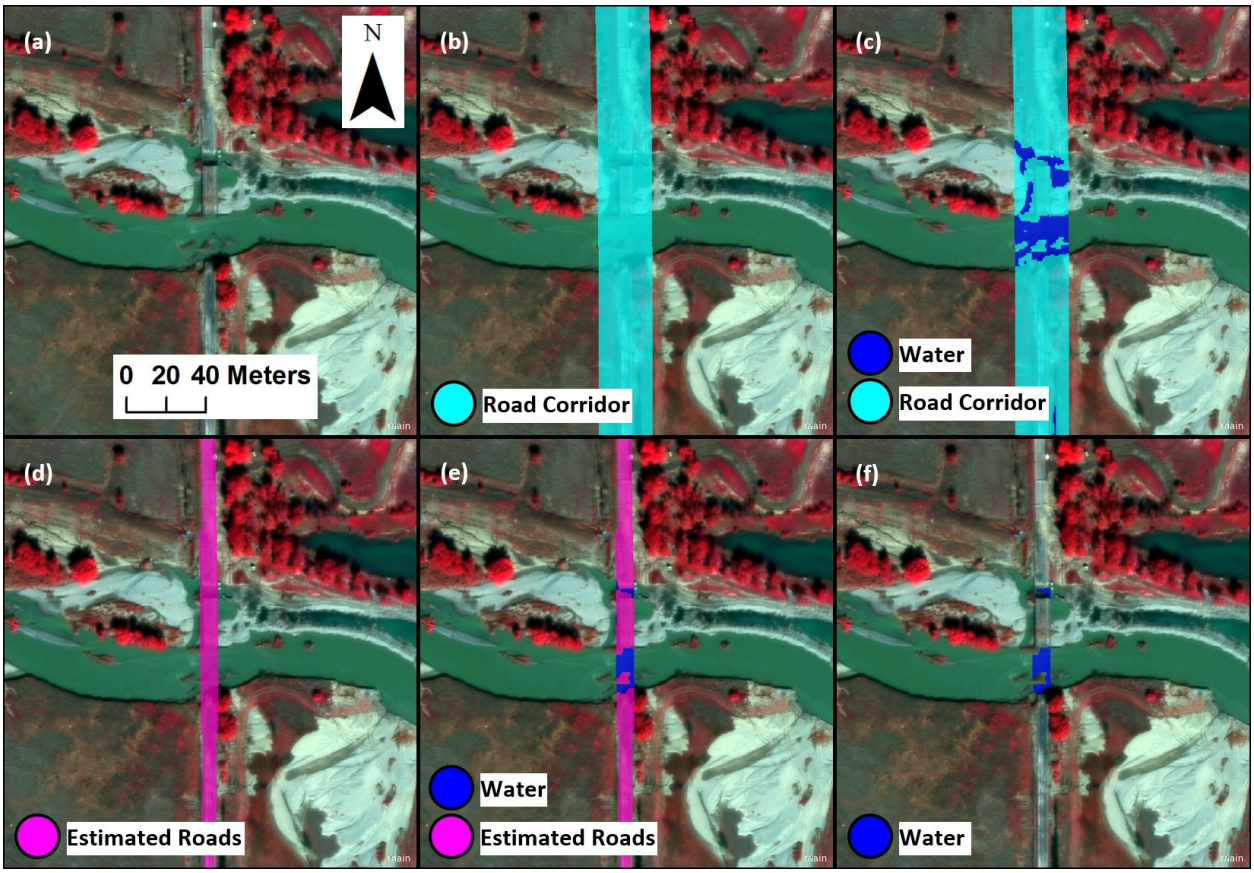

Figure 2. Modeling flow for automated feature extraction of flood-related damage in Longmont, Colorado, September 2013. WorldView-2 imagery acquired post-storm was imported into eCognition (a), along with publicly-accessible road centerlines. The road centerlines were used to model road corridors (b), and the Near Infrared band of the WorldView-2 imagery was used to identify water (c). The initial classification was refined by estimating actual road surfaces (d) and then adding the water that covered them, wholly or in part (e). The final step was to evaluate the size and shape of the water features, eliminating objects that were small and had proportionately large borders with the road edge (f).

Data Export

Transportation breaks identified by OBIA modeling were outputted into two GIS-ready formats: 1) ArcGIS shapefiles; and 2) ERDAS Imagine (Intergraph) rasters. Depending on end-user preference, output for individual tiles could then be mosaicked into seamless layers or used individually, permitting display or query in a GIS software program. For non-technical end-users, road disruptions were also highlighted by creating JPEG snapshots showing individual breaks and the WorldView-2 imagery that was used to identify them. Each JPEG was named according to the projection coordinates for the centroid of each scene (e.g., X489689Y4445541.jpg) and then displayed in Google Maps (Google), an online mapping utility with easy-to-use navigation and query capabilities. An example of flood-related transportation break in Longmont, Colorado, as displayed in Google Maps, is shown in Figure 5.

RESULTS, DISCUSSION, AND CONCLUSIONS

The floodwaters model produced 18 damage occurrences for Longmont, Colorado; review of the snapshots for these occurrences indicated that 78% (14) were legitimate road disruptions. Most of the network breaks involved residual flooding that had not yet receded when the imagery was acquired, but washed out bridges and partially-eroded roadbeds were also captured. The false positives included a river flowing under an intact railroad bridge, standing

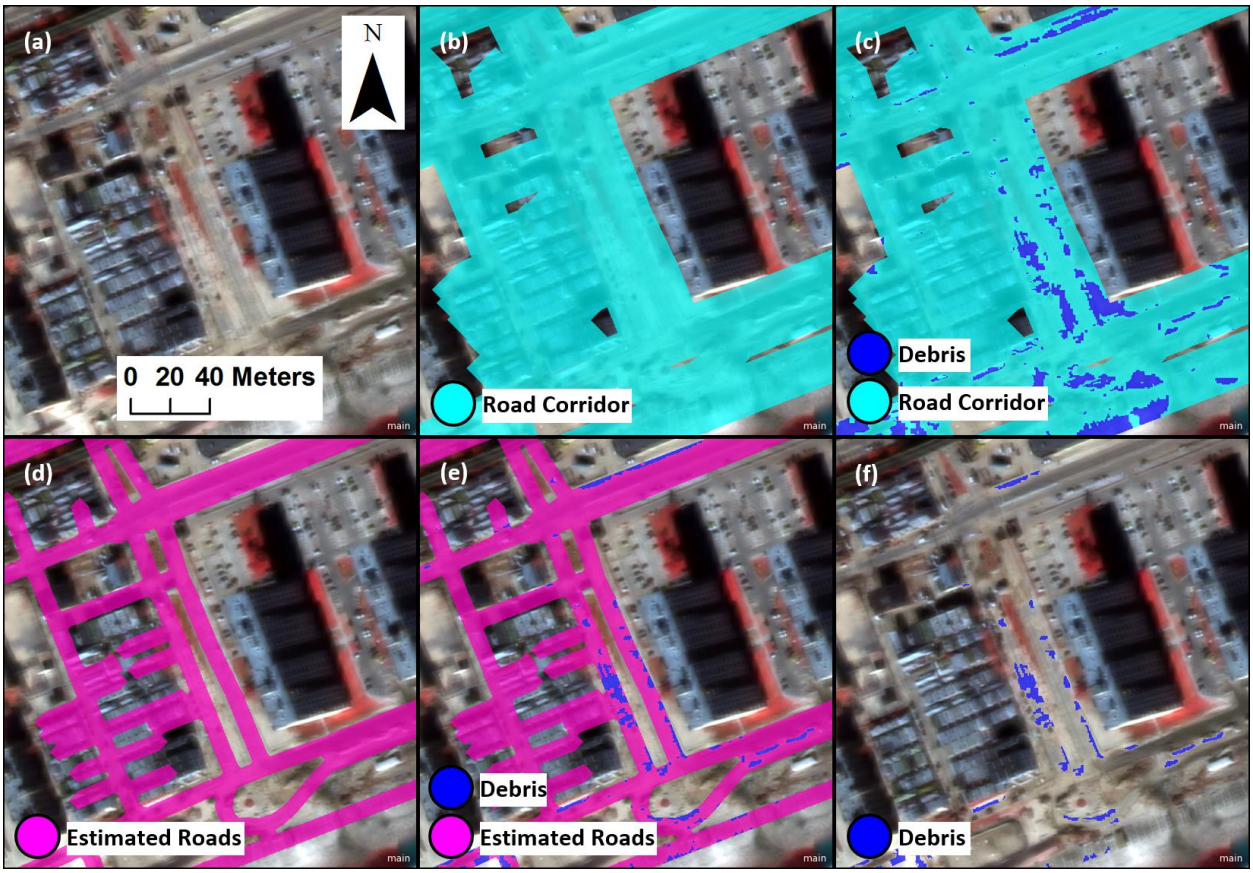

Figure 3. Modeling flow for automated feature extraction of debris deposited by the storm surge associated with Hurricane Sandy, New York City, November 2012. WorldView-2 imagery acquired post-storm was imported into eCognition (a), along with publicly-accessible road centerlines. The road centerlines were used to model road corridors (b), and a combination of Visible Brightness and the Normalized Difference Vegetation Index (NVDI) calculated from the WorldView-2 imagery was used to identify debris (c). The initial classification was refined by estimating actual road surfaces (d) and then adding the debris that covered them, wholly or in part (e). The final step was to evaluate the size and shape of the debris features, eliminating objects that were small and had proportionately large borders with the road edge (f).

water adjacent to roads that did not affect traffic, and standing water in a partially-completed subdivision where the available road centerline layer did not match the WorldView-2 imagery (i.e., the road centerline layer included a road that had not yet been constructed when the imager was acquired). Rule-set processing for the Longmont area required 26 min. using 5 processing cores, covering a study area of 22,098ha (54,604ac). The debris model was less effective; review of the JPEG snapshots indicated that 105 of 214 (49%) occurrences contained actual disruptions, usually a layer of sand deposited by the receding storm surge. The false positives were most often impervious surfaces unaffected by the storm surge or tall buildings exhibiting noticeable distortion in non-orthorectified imagery. In New York City's densely-clustered urban environment, distorted buildings with bright rooftops leaning into adjacent roadways were occasionally captured within the widths of estimated road surfaces. The debris model required 17 min. of processing time using 5 cores to cover a study area of 10,150ha (25,080ac).

Both models over-predicted storm-related damage, but this was partly by design as errors of commission are less severe than errors of omission. Storm damage can vary greatly in severity and extent, and the overall goal was to capture as many candidate disruptions as possible, recognizing that a human analyst will have to provide a final assessment. The export products from eCognition permitted fast and efficient review of candidate sites, especially when combined with commonly-available web-mapping utilities. Individual sites that require additional review could then be queried in depth, either with the available imagery or in the field. The magnitude of over-prediction by the debris model was also anticipated, given the fundamental difficulty in discriminating exposed soil from impervious

surfaces with similar spectral properties. As a first cut, the debris model greatly narrowed the range of potential damage occurrences in the study area, despite

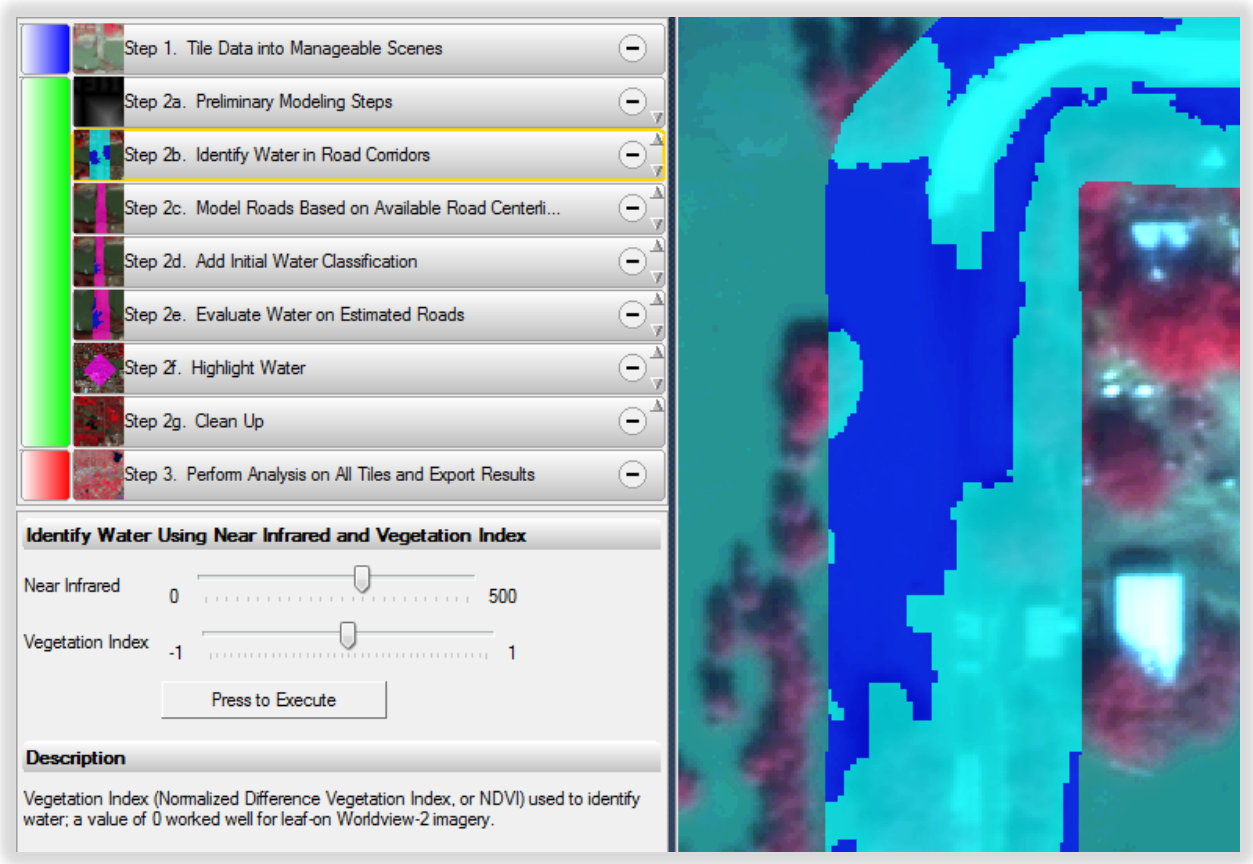

Figure 4. Simplified graphic-user interface for the floodwaters model in eCognition Architect. Rather than direct manipulation of the underlying rule set, the Architect application permits rapid analysis of most-disaster imagery using buttons and slider bars.

the number of erroneous sites, and the snapshots showing buildings and legitimate impervious surfaces were then reviewed and quickly culled from the set of candidate sites requiring further examination.

Automated processing could nonetheless be improved by incorporating additional contextual criteria that help discriminate false positives from actual road disruptions, especially in the debris model. For example, a distance function could be applied to debris classification, limiting analysis to roads within a specific distance of the immediate shoreline, and the distance to other modeled debris could be used to eliminate small, isolated occurrences. Contextual discrimination of candidate sites would also benefit from incorporation of additional input datasets such as LiDAR and other thematic datasets (e.g., building footprints, roadbed polygons, hydrology), where available. However, use of these additional datasets would have to be balanced with the necessity of maintaining efficient, simple models; more complex and data-rich processing would likely require more time and technical expertise, two resources that may be in short supply in the immediate aftermath of a damaging storm. Similarly, the debris model for New York City would undoubtedly benefit from use of orthorectified images in which building lean has been partially or wholly corrected, but the resources needed to orthorectify them may be unavailable to damage-assessment teams.

The models described here thus represent a compromise between discriminatory power and speed and ease of use. Human cognition and synthesis are still needed to categorize and rank damage sites, and to prioritize effective emergency response. However, automated feature extraction with eCognition provides an effective method for simplifying initial analysis and highlighting potential damage, capitalizing on the availability of high-resolution imagery and giving first responders essential information in their efforts to understand and address storm-related transportation disruptions.

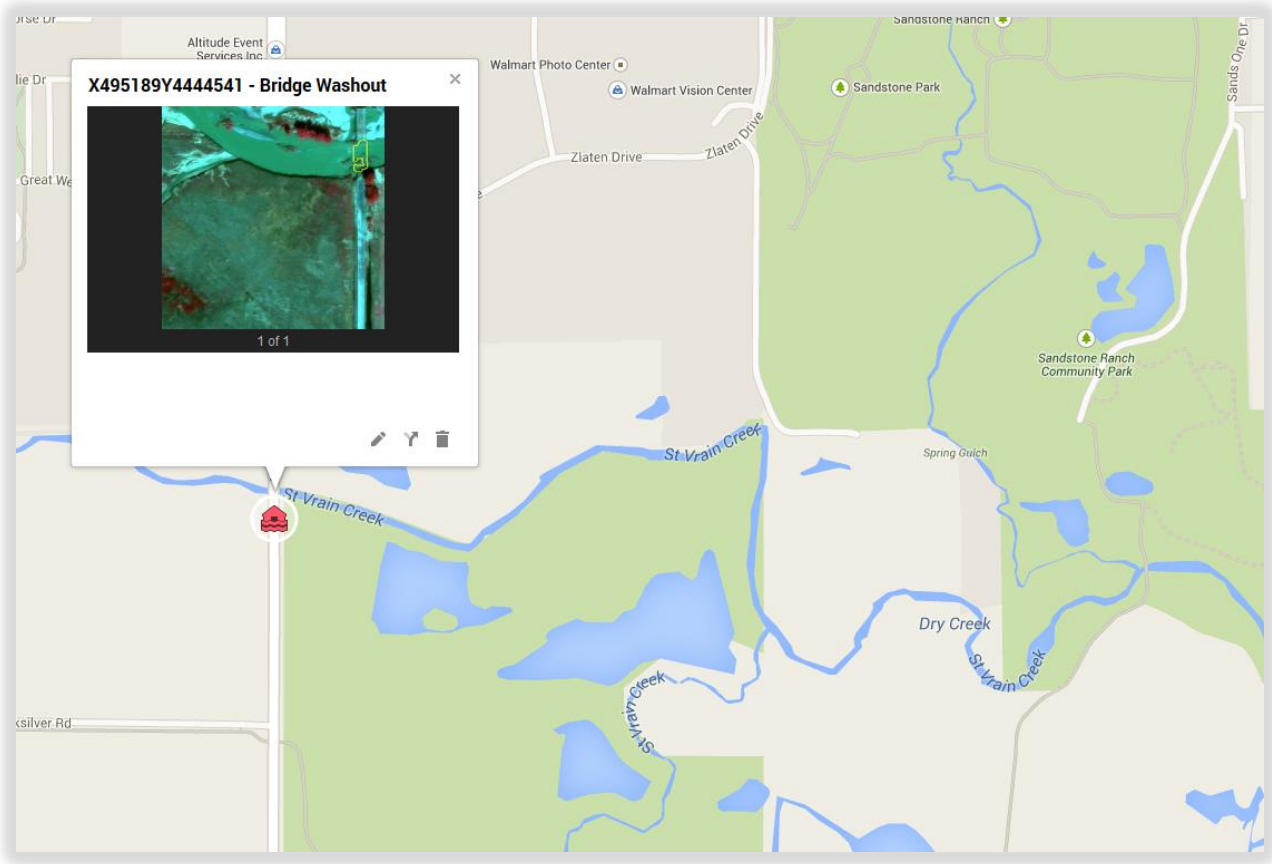

Figure 5. Query and display of eCognition modeling output for flood-related transportation damage in Longmont, Colorado, September 2013, in Google Maps.

ACKNOWLEDGMENTS

This work was funded by the U.S. Department of Transportation under grant RITARS-12-H-UVM. We are grateful to Digital Globe for providing imagery to support this work and Trimble for providing eCognition software.

DISCLAIMER: The views, opinions, findings and conclusions reflected in this presentation are the responsibility of the authors only and do not represent the official policy or position of the USDOT/OST-R, or any State or other entity.

REFERENCES

Barrington, L., S. Ghosh, M. Greene, S. Har-Noy, J. Berger, S. Gill, A. Yu-Min Lin, and C. Huyck. 2011. Crowdsourcing earthquake damage assessment using remote sensing imagery. *Annals of Geophysics* 54(6):680-687. doi:10.4401/ag-5324

Benz, U.C., P. Hofmann, G. Willhauck, I. Lingenfelder, and M. Heynen. 2004. Multi-resolution, object-oriented fuzzy analysis of remote sensing data for GIS-ready information. *ISPRS Journal of Photogrammetry and Remote Sensing* 58(3-4):239-258. doi:10.1016/j.isprsjprs.2003.10.002

Bessis, J.-L., J. Béquignon, and A. Mahmood. 2003. The International Charter "Space and Major Disasters" initiative. *Acta Astronautica* 54:183-190. doi:10.1016/S0094-5765(02)00297-7

Bessis, J.-L., J. Béquignon, and A. Mahmood. 2004. Three typical examples of activation of the International Charter "Space and Major Disasters." *Advances in Space Research* 33:244-248. doi:10.1016/S0273-1177(03)00467-8

Ehrlich, D., H.D. Guo, K. Molch, J.W. Ma, and M. Pesaresi. 2009. Identifying damage caused by the 2008 Wenchuan earthquake from VHR remote sensing data. *Internal Journal of Digital Earth* 2(4):309-326. doi: 10.1080/17538940902767401

Gitas, Z., A. Polychronaki, T. Katagis, and G. Mallinis. Contribution of remote sensing to disaster management activities: a case study of the large fires in the Peloponnese, Greece. *International Journal of Remote Sensing* 29(6):1847-1853. doi:10.1080/01431160701874553

Ito, A. 2005. Issues in the implementation of the International Charter on Space and Major Disasters. *Space Policy* 21:141-149. doi:10.1016/j.spacepol.2005.02.003.

MacFaden, S. W., J. P. M. O'Neil-Dunne, A. R. Royar, J. W. T. Lu, and A. G. Rundle. 2012. High-resolution tree canopy mapping for New York City using LIDAR and object-based image analysis. *Journal of Applied Remote Sensing* 6(1): 063567–1–063567–23. doi:10.1117/1.JRS.6.063567

O'Neil-Dunne, J.P.M., S.W. MacFaden, and K.C. Pelletier. 2011. Incorporating contextual information into object-based image analysis workflows. *Proceedings of the American Society for Photogrammetry and Remote Sensing (ASPRS) 2011, Annual Conference*, Milwaukee, WI, 11p.
URL: http://info.asprs.org/publications/proceedings/Milwaukee2011/files/ONEILDUNNE.pdf

O'Neil-Dunne, J., S. MacFaden, and A. Royar. 2014. A versatile, production-oriented approach to high-resolution tree-canopy mapping in urban and suburban landscapes using GEOBIA and data fusion. *Remote Sensing* 6:12837-12865. doi:10.3390/rs61212837

Stryker, T., and B. Jones. Disaster response and the International Charter Program. *Photogrammetric Engineering & Remote Sensing* 75(12):1342-1344.
URL:http://asprs.org/a/publications/pers/2009journal/december/highlight.pdf

Voigt, S., T. Schneiderhan, A. Twele, M. Gahler, E. Stein, and H. Mehl. 2011. Rapid damage assessment and situation mapping: learning from the 2010 Haiti earthquake. *Photogrammetric Engineering & Remote Sensing* 77(9):932-931. URL: http://core.ac.uk/download/pdf/11152364.pdf